

Ocean Climate Drift and Interdecadal Oscillation Due to a Change in Thermal Damping

WENJU CAI

CSIRO Division of Atmospheric Research, Aspendale, Victoria, Australia

PETER C. CHU

Department of Oceanography, Naval Postgraduate School, Monterey, California

(Manuscript received 27 November 1995, in final form 24 April 1996)

ABSTRACT

The authors investigate the effect of a change in the rate of thermal damping upon the climate of an ocean general circulation model. Initially, the thermal forcing condition is that proposed by Haney, that is, restoring the model surface temperature to a climatology. The restoring condition represents a strong damping. When a steady state is reached, the thermal damping is switched to a weaker one, but the atmosphere-ocean heat exchange is adjusted so that at the moment of the switch the heat flux is identical to that prior to the switch. It is found that interdecadal oscillations and climate drift occur as a result of the switch, regardless of the forcing condition for salinity. The cause for the variability and drift can be traced to the spinup. During the spinup, the surface climatology of the model ocean is forcefully "nudged" toward that of the climatology, regardless of whether or not the internal dynamics of the model ocean can maintain the climatology. This leads to intermittent convections in the spinup state. When the thermal damping becomes weaker, the system chooses a convective pattern (the location and intensity of the convection) more compatible with the internal dynamics. An implication of these results is that drift and variability in a coupled model may be caused by the mechanism. Effects of flux corrections in coupled models are discussed.

1. Introduction

In atmosphere-ocean coupling, a precoupling spinup is often carried out to provide initial conditions and to derive flux corrections. During this spinup, strong restoring forces on both temperature and salinity are usually used in order to best represent the current ocean climate. These represent strong thermal and saline damping. (Ocean modelers often refer to such a procedure as a strong coupling because the surface ocean conditions are strongly constrained by the atmospheric conditions represented by the restoring forcings.) Upon switching from restoring boundary conditions to an active atmosphere, the damping through saline forcing weakens and the interaction between freshwater flux and sea surface salinity (SSS) becomes indirect and nonlinear, mostly via the dependence of evaporation upon sea surface temperature.

Based on such a change, many studies have examined the effect of a change of the saline forcing from a restoring to a flux condition, while maintaining the restoration for temperature (e.g., Bryan 1986; Marotzke 1990; Marotzke and Willebrand 1991;

Weaver and Sarachik 1991a,b; Moore and Reason 1993; Zhang et al. 1993; Power and Kleeman 1993; Power et al. 1994; Huang 1994; Power 1995; Cai and Godfrey 1995; Cai 1995a,b). This set of forcing conditions is often called "mixed boundary conditions." These previous studies have revealed interesting features of the thermohaline circulation, including a polar halocline catastrophe (Bryan 1986), a flush (Marotzke 1989; Weaver and Sarachik 1991b), low-frequency oscillations (Marotzke 1989), and oscillations on decadal timescale (Weaver and Sarachik 1991a,b; Cai 1995a). Further, the thermohaline circulation is extremely sensitive to perturbations in the freshwater flux. A small perturbation can "flip" the ocean circulation from an equilibrium with a northern sinking cell to one without (Marotzke 1990; Marotzke and Willebrand 1991; Hughes and Weaver 1994), and a substantial drift can be induced by noise in the freshwater flux (Power 1995).

It is now clear that when the thermal forcing is switched to that provided by an active atmosphere the thermal damping is also weakened (Zhang et al. 1993; Moore and Reason 1993; Mikolajewicz and Maier-Reimer 1994; Marotzke 1994; Rahmstorf and Willebrand 1995; Cai and Godfrey 1995). In particular, Marotzke (1994) suggested that the thermal damping rate is about $12 \text{ W m}^{-2} \text{ K}^{-1}$, rather than the commonly used $30\text{--}50 \text{ W m}^{-2} \text{ K}^{-1}$. This is confirmed by Rahmstorf

Corresponding author address: Dr. Wenju Cai, Division of Atmospheric Research, CSIRO, Private Bag 1, Mordialloc, Victoria 3195, Australia.

Report Documentation Page

Form Approved
OMB No. 0704-0188

Public reporting burden for the collection of information is estimated to average 1 hour per response, including the time for reviewing instructions, searching existing data sources, gathering and maintaining the data needed, and completing and reviewing the collection of information. Send comments regarding this burden estimate or any other aspect of this collection of information, including suggestions for reducing this burden, to Washington Headquarters Services, Directorate for Information Operations and Reports, 1215 Jefferson Davis Highway, Suite 1204, Arlington VA 22202-4302. Respondents should be aware that notwithstanding any other provision of law, no person shall be subject to a penalty for failing to comply with a collection of information if it does not display a currently valid OMB control number.

1. REPORT DATE 24 APR 1996		2. REPORT TYPE		3. DATES COVERED 00-00-1996 to 00-00-1996	
4. TITLE AND SUBTITLE Ocean Climate Drift and Interdecadal Oscillation Due to a Change in Thermal Damping				5a. CONTRACT NUMBER	
				5b. GRANT NUMBER	
				5c. PROGRAM ELEMENT NUMBER	
6. AUTHOR(S)				5d. PROJECT NUMBER	
				5e. TASK NUMBER	
				5f. WORK UNIT NUMBER	
7. PERFORMING ORGANIZATION NAME(S) AND ADDRESS(ES) Naval Postgraduate School, Department of Oceanography, Monterey, CA, 93943				8. PERFORMING ORGANIZATION REPORT NUMBER	
9. SPONSORING/MONITORING AGENCY NAME(S) AND ADDRESS(ES)				10. SPONSOR/MONITOR'S ACRONYM(S)	
				11. SPONSOR/MONITOR'S REPORT NUMBER(S)	
12. DISTRIBUTION/AVAILABILITY STATEMENT Approved for public release; distribution unlimited					
13. SUPPLEMENTARY NOTES					
14. ABSTRACT					
15. SUBJECT TERMS					
16. SECURITY CLASSIFICATION OF:			17. LIMITATION OF ABSTRACT	18. NUMBER OF PAGES	19a. NAME OF RESPONSIBLE PERSON
a. REPORT unclassified	b. ABSTRACT unclassified	c. THIS PAGE unclassified			

and Willebrand (1995) in an ocean-only model forced by a thermal-energy-balanced atmosphere model. Hence, it is equally important to study the effect of a change in thermal damping because all coupled models, flux corrected or not, go through such a change when coupling occurs.

Most of the coupled atmosphere–ocean–sea ice models (e.g., Manabe and Stouffer 1993, 1994; Cubasch et al. 1994; Gordon and O’Farrell 1996, hereafter GOF) employ a “flux correction” technique (Sausen et al. 1988; Sausen and Lunkeit 1990; Moore and Gordon 1994) to avoid “climate drift,” which is the trend of each model component with time after coupling, toward a climatology significantly different from that prior to coupling. The flux correction fields to the ocean model are usually obtained and applied in the following way. The ocean component is spun up under restoring boundary conditions (Haney 1971), which force the model toward SST and SSS climatologies, and the implied fluxes required for maintaining these climatologies are diagnosed. Similarly, the atmospheric component is spun up under the influence of the same climatologies, and another set of implied freshwater and heat exchange with the ocean is diagnosed. The difference between these fluxes is the flux correction; this is applied during subsequent coupled experiments. This technique in effect ensures that *at the moment of coupling* the ocean receives heat and freshwater fluxes approximately the same as those prior to the coupling. Thereafter, the total flux is varying according to the dynamics of the coupled system.

However, the correction does not fully prevent drift, particularly at high latitudes (e.g., Figs. 5 and 6 of GOF). Further, upon coupling, oceanic variabilities of interdecadal timescale occur (Delworth et al. 1993). An examination of this issue requires an understanding as to what may induce such oscillations and anomalous drift. In this study, we suggest that a possible cause for drift and variability is the change in the rate of thermal damping.

The structure for the rest of this paper is as follows. In section 2, the ocean general circulation model (OGCM) and the thermal forcing condition are described. In section 3, results are presented showing how drift and variability are induced by a change in thermal damping. Some related issues are addressed in section 4. In section 5, major conclusions are presented and the implications for atmosphere–ocean coupled modeling are discussed.

2. The model and the thermal forcing condition

This study employs the Pacanowski et al. (1991) version of the Bryan–Cox–Semtner OGCM, which is based on the work of Bryan (1969). The model has a width of 60° and a length of 144° extending from 72°S to 72°N. The Southern Hemisphere includes a modeled Antarctic Circumpolar Current (ACC) passage from

44° to 60°S and a sill 2350 m deep in the model’s Drake Passage; elsewhere it is flat bottomed. This sill is intended to provide a realistic ACC transport through the setup of a bottom pressure difference between the two sides of the passage (Holland 1973; Gill and Bryan 1971; Cai 1994; Cai and Baines 1996). Otherwise, the flat bottom would lead to an unrealistically large wind-driven ACC. The horizontal grid spacing is 4° latitude by 4° longitude. The model has 12 levels in the vertical, and the depth distribution is listed in Table 1. The model uses the Cox (1987) parameterization to compute vertical diffusion and convection implicitly. The enhanced vertical diffusivity in regions of static instability is set at $10^5 \text{ cm}^2 \text{ s}^{-1}$, which is the convective adjustment in the model.

Suppose a restoring spinup is carried out in which the model SST is restored to T_a , and the steady-state solution has an SST field T_s and a heat flux field F_{spin} . They satisfy

$$F_{\text{spin}} = K_H(T_a - T_s). \quad (1)$$

Here K_H is the damping rate during the spinup. The thermal forcing is then switched to

$$Q_{ao} = K_r(T_r - T_1) \quad (2)$$

to achieve a weaker damping. Here K_r is the new damping rate ($K_r < K_H$), T_r is the new restoring temperature, and T_1 is the temperature of the uppermost level.

The T_r field is diagnosed from the spinup state by setting

$$K_r(T_r - T_s) = F_{\text{spin}} \quad (3)$$

so that at the moment of the switching only the damping rate changes: the heat flux is exactly the same as that prior to the switch. As in a flux-corrected coupled model, the heat flux is subsequently allowed to change. The simplicity of such a treatment of the forcing condition allows an examination of the effect of a change in the rate of thermal damping *alone*.

The physics behind this treatment of surface thermal forcing can be realized from a simple coupled system

TABLE 1. Distribution of vertical levels.

Level	Thickness (m)	Depth of T, S (m)
1	25.0	12.5
2	25.0	37.5
3	40.0	70.0
4	70.0	125.0
5	110.0	215.0
6	200.0	370.0
7	330.0	635.0
8	450.0	1025.0
9	650.0	1575.0
10	900.0	2350.0
11	900.0	3250.0
12	900.0	4150.0

consisting of a simple atmosphere (Schopf 1983; Sausen et al. 1988; Zhang et al. 1993; Cai and Greatbatch 1995) and a mixed layer ocean. The heat balance for the atmosphere is

$$0 = -K_H(T_a - T_1) - K'_r T_a + Q_a \quad (4)$$

and for the mixed layer ocean is

$$C_o \frac{\partial T_1}{\partial t} = K_H(T_a - T_1) + Q_o. \quad (5)$$

Equation (4) expresses a balance between heat transfer from the ocean to the atmosphere given by the $-K_H(T_a - T_1)$ term, heat loss to space given by $-K'_r T_a$, and heat sources due to solar input and the divergence of the atmospheric heat transport given by Q_a . Here, K'_r is the atmospheric radiative feedback parameter, C_o is the specific heat capacity of the mixed layer ocean, and Q_o is the oceanic heat source.

Defining a temperature

$$T_r = Q_a / K'_r, \quad (6)$$

we can write (4) as

$$0 = -K_H(T_a - T_1) + K'_r(T_r - T_a). \quad (7)$$

From (7), expressing T_a in terms of other quantities and substituting into (5), we have

$$C_o \frac{\partial T_1}{\partial t} = K_r(T_r - T_1) + Q_o, \quad (8)$$

where

$$K_r = \frac{K_H K'_r}{(K_H + K'_r)}. \quad (9)$$

A comparison of (5) and (8) indicates that (2) represents a simple coupling [see Zhang et al. (1993) for a detailed discussion]. Since K'_r is a factor of about 20 less than K_H (Dickinson 1981), it follows from (9) that K_r is also much smaller than K_H . Thus, switching from restoring forcing to (2) leads to a weaker thermal damping. In (2) T_r is kept constant. This means that Q_a is fixed [see Eq. (6)]. The physical implication is that the atmospheric heat transport under the new forcing is exactly the same as that implied by the steady state of the spinup.

Defining a ratio

$$\alpha = K_r / K_H \quad (\alpha < 1), \quad (10)$$

which measures the change in thermal damping, we can rewrite the new forcing [i.e., (2)], using (1) and (3), as

$$\begin{aligned} & K_r(T_r - T_1) \\ &= K_r(T_r - T_s) - K_r(T_a - T_s) + K_r(T_a - T_1) \\ &= (1 - \alpha)F_{\text{spin}} + \alpha K_H(T_a - T_1). \end{aligned} \quad (11)$$

Thus, the new forcing is equivalent to a part of the constant diagnosed heat flux plus a weaker restoring forcing.

3. Model results

a. Change of thermal damping from a spinup under restoring conditions on both temperature and salinity

The OGCM is spun up by restoring the uppermost level temperature and salinity to a zonally uniform temperature and salinity, given by the profiles shown in Fig. 1. These approximate the zonally averaged value of the observed fields. The e -folding restoring time is 30 days for salinity and 15 days for temperature, the latter corresponding to a thermal damping rate K_H of $79 \text{ W m}^{-2} \text{ }^\circ\text{C}^{-1}$. We choose a longer timescale for salinity to produce a freshwater flux with more realistic magnitudes. This prevents a collapse of the overturning circulation upon switching to mixed boundary conditions (Tziperman et al. 1994; Cai 1996a). The model is also subject to the wind stress used by Bryan (1987). Only during the first 11 000 years (88 000 years at the bottom level) of the spinup is the acceleration of Bryan (1984) used. By then, the spinup reaches a statistically steady state. Then, the integration is extended for another 1000 years without the acceleration for a final steady state. The overturning circulation is shown in Fig. 2 and is qualitatively similar to that in the real Atlantic. It features a northern sinking cell, similar to the North Atlantic Deep Water formation (NADWF) cell and an Antarctic Circumpolar Current convective cell. The model ACC during the spinup reaches 102 Sv ($\text{Sv} \equiv 10^6 \text{ m}^3 \text{ s}^{-1}$).

In run 1 (Table 2), the thermal damping rate is switched to $K_r = 19.75 \text{ W m}^{-2} \text{ }^\circ\text{C}^{-1}$ (corresponding to a damping timescale of 60 days), with the forcing given by (2) and T_r diagnosed from the steady state in terms of (3). In this case, $\alpha = 0.25$, and from (11) the new forcing consists of 75% of the diagnosed heat flux and 25% of the restorative forcing used in the spinup. The restoration for salinity is maintained. It is relevant to note that a flux correction for coupled models is usually diagnosed by averaging the flux fields over a period of several years. This does not ensure an identical heat flux at the moment of the switch and may exert effect on the subsequent model solution. In order to eliminate this effect in the present study, such an average is not carried out.

The model is integrated for a further 11 000 years. Strong drift occurs as can be seen from Fig. 3, which shows the time series of the overturning sampled at latitude 60°N , depth 2350 m. Unless otherwise stated, single-point time series of overturning are all taken at this location. Several features emerge. First, the new steady-state drifts from the spinup state, and the largest timescale for the drift reaches several thousands of

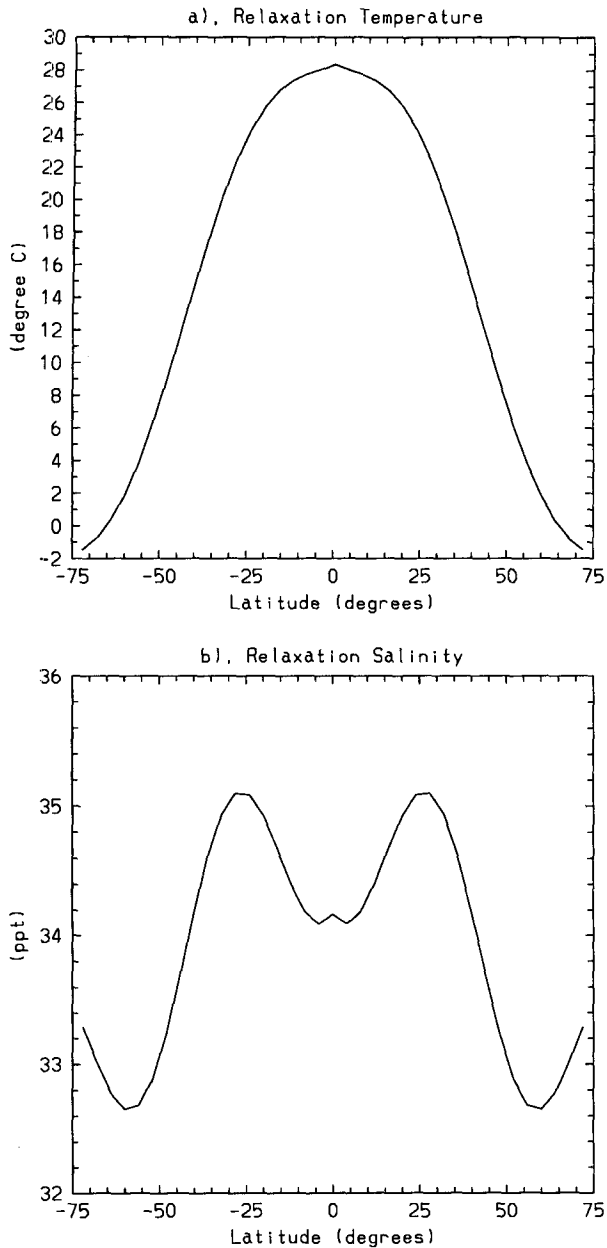


FIG. 1. (a) Surface relaxation temperature (in $^{\circ}\text{C}$) and (b) surface relaxation salinity (in parts per thousand).

years. Second, some variabilities, apparently thermally driven, are induced at initial stage. When the thermal damping is weakened further, to $K_r = 9.875 \text{ W m}^{-2} \text{ }^{\circ}\text{C}^{-1}$ ($\alpha = 0.125$), giving rise to run 2 (Table 1), regular thermal oscillations with a period of 26 years occur (Fig. 4). The characteristics of the oscillation are given in Greatbatch and Zhang (1995) and Cai et al. (1995) and will not be repeated here. As in these studies, the oscillation reproduced some important features of the variability seen in the Geophysical

Fluid Dynamical Laboratory (GFDL) coupled model (Delworth et al. 1993).

An examination reveals that the location of the maximum overturning of run 1 shifts away from that of the spinup and the maximum decreases by about 0.5 Sv. This drift significantly modifies the temperature field, especially the SSTs (Fig. 5a). This modification is associated with the T_r field (Fig. 5b) and changes in the convective pattern (Figs. 5c and 5d). By convection pattern we mean the location and intensity (the penetration depth) of the convection. In order to maintain the convection pattern of the spinup, T_r over the convective regions is "corrected" to be fairly cold in order to allow heat loss. Once the convection pattern (location and intensity) changes, this cold bias becomes the cause for drift. For example, under the weaker damping, convection in the northeastern corner weakens, and some even cease, but the low value of T_r in that region still allows large heat loss. This leads to a drop in SST. A similar process takes place in the eastern side of the model Weddell Sea, and the cold water appears to spread along the model ACC. By contrast, convection off the northern western boundary intensifies, where T_r is not low enough to remove the associated heat transported from below by the intensified convection. This leads to a strong warming there. This process is also present in run 2, where the convection pattern changes periodically (Fig. 6).

Instability of the convection pattern of the spinup state is a major feature associated with the drift. This is supported by Fig. 5a, which shows that the largest drifts occur over convective regions. What causes the instability? In a study on the effect of a change in saline damping using a low-resolution model with realistic topography, Moore and Reason (1993) discussed the source of drift and variability in their model. The so-called equilibrium solution of the spinup via relaxation to a given climatology is not a perfect steady-state solution of the model equations. In areas characterized by sharp oceanic fronts and high convective activity, the model, due to the limitation of model dynamics, cannot maintain the climatology. Therefore, in these areas the

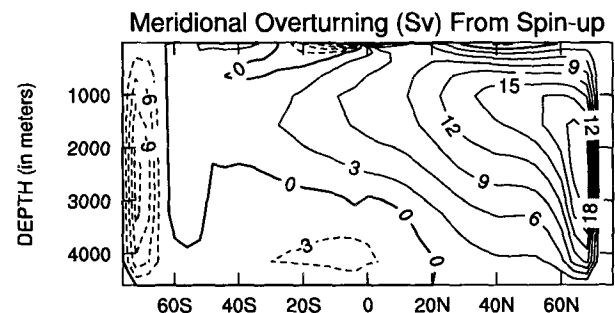


FIG. 2. Overturning streamfunction (in Sverdrups) from the spinup (run RR) under restoring boundary conditions for temperature and salinity.

TABLE 2. Details of main model experiments. The thermal forcing condition is either a restoring with the restoring time (in days) indicated in parentheses or that described by Eq. (11), that is, a restoring plus a portion of a diagnosed flux. The saline forcing condition is either a restoring or diagnosed flux. In the thermal-only cases, the salinity forcing is zero.

Run	Initial condition	Thermal forcing	Saline forcing	Characteristics
RR	Rest	Restoring (15 d)	Restoring (30 d)	Steady
1	RR	Restoring (60 d) + Flux	Restoring (30 d)	Steady, drift from RR
2	RR	Restoring (120 d) + Flux	Restoring (30 d)	Oscillatory, drift from RR
RF	RR	Restoring (15 d)	Flux	Steady
3	RF	Restoring (120 d) + Flux	Flux	Oscillatory, drift from RF
R0	Rest	Restoring (15 d)	(Thermal only)	Steady
4	Rest	Restoring (30 d) + Flux	(Thermal only)	Steady, drift from R0
5	Rest	Restoring (45 d) + Flux	(Thermal only)	Oscillatory, drift from R0

model is systematically biased away from the climatology, and the surface heat and salinity fluxes tend to oscillate about some mean value. This idea was supported by time series of the global average fluxes, which show that as the imperfect steady state is approached, the global average oceanic surface heat and salt fluxes possess a significant oscillatory component. Similar time series from our spinup confirm theirs. The oscillatory feature continues to be present even if our model is integrated for a further 10 000 years.

During the spinup, SSTs are forcefully "nudged" to the prescribed values, in a similar way to some data assimilation studies. In areas where the model is not compatible with the climatology it tries to resist the restoring (nudging) conditions at the surface through the action of dynamic adjustment [see Moore and Reason (1993) and the references therein]. The adjustment process, however, never reaches completion because the restoring conditions constantly damp it. The restoring boundary conditions therefore act as a "brake" on the dynamic adjustment process and suppress the "incompatibility." This leads to intermittent convections of the spinup steady state.

Once the surface restoring condition on temperature is switched to a weak restoring condition (weak damping), temperature anomalies in areas with incompatibility are freer to evolve. In other words, the internal model dynamics is allowed to play a greater role in determining the convection. The intermittent convections of the spinup state change their location and penetration depth. This leads to the drift.

If the drift is substantial, it influences the convection pattern in turn and produces oscillations, a periodic process in which the anomaly associated with the drift and the change in the convection pattern each become the cause for the other. This can be understood via the advective process (Huang and Chou 1994; Greatbatch and Zhang 1995; Cai et al. 1995). Suppose that at a location a negative SST anomaly develops due to drift. The anomaly enhances convection, and more subsurface heat is transmitted to the surface. If the surface cooling is not strong enough to remove the additional heat, a positive SST anomaly is produced. The positive

SST anomaly then reduces the convection, and SST drops, owing not only to the weakened subsurface heating but also to the surface cooling. Consequently, a negative SST anomaly develops. In this way, the cycle repeats itself, provided that the damping is weak. Alternatively, the oscillation can be understood via the thermohaline adjustment considered by Wajsovicz and Gill (1986) in terms of boundary waves. This process was recently revisited by Winton (1996) and Greatbatch and Paterson (1996). These authors find that an anomalous northward flow associated with a stronger overturning pumps a heat anomaly into the northeastern corner. The anomaly then propagates westward along the northern boundary by means of a boundary wave. Much of the time in an oscillation cycle is spent at the northern boundary, where the weak vertical stratification slows the propagation of boundary waves, leading to the emergence of an interdecadal timescale.

In assessing the relevance of our model results to oscillations in a coupled model, we note that in a coupled model atmospheric changes also take place. These atmospheric changes are likely to play a role in generating oscillations. This is proposed by Griffies and Tziperman (1995) in a box model study as a cause for the oscillation in the GFDL coupled model (Delworth et al. 1993). Their result suggests that the variability in the coupled model is externally driven rather than being an internal oceanic process, as discussed in the last paragraph. Clearly, there is a need to reconcile these results. It is likely that in a coupled system these processes coexist. This is an important aspect that needs further study.

Returning to the drift and the oscillation in the present study, we note that our results are in sharp contrast to those of Sausen et al. (1988), who reported that when a heat flux correction was employed and the restoration for salinity was maintained, no drift occurred. It is important to point out that their model spinup was in a perfect steady state; hence, there was no internal variability that could grow upon the change in the thermal damping. In our model drifts occur regardless of the forcing condition for salinity. This can be seen from the following manipulation:

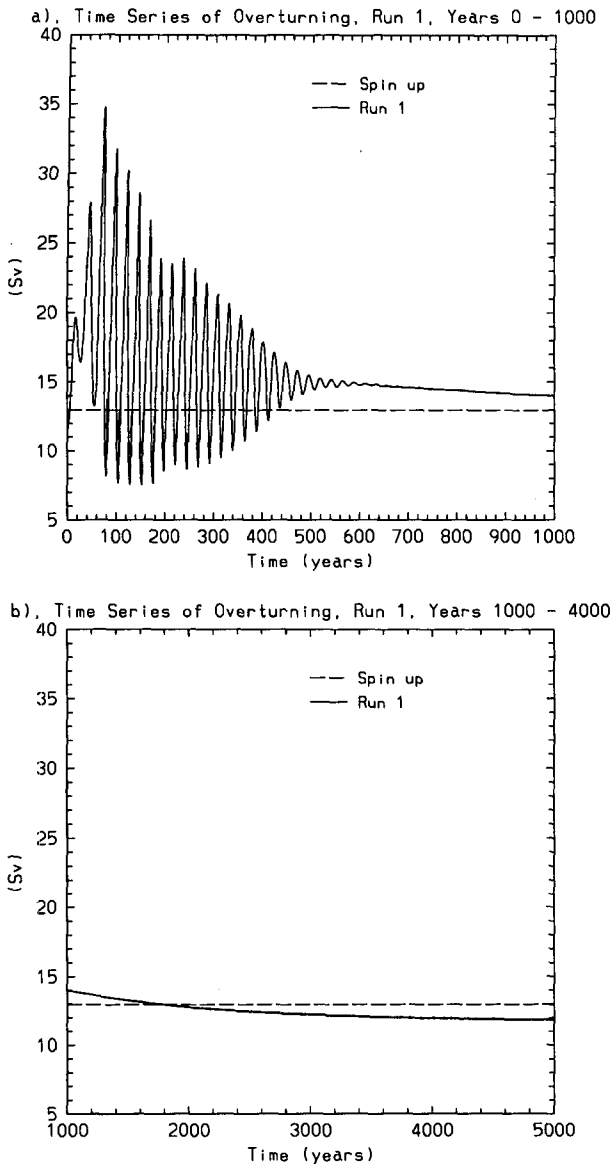


FIG. 3. Time evolution of the northern overturning (in Sverdrups) at a location of 64°N , 2350 m for run 1, that is, with a thermal damping of $19.75 \text{ W m}^{-2} \text{ K}^{-1}$ and a restoration on surface salinity, for (a) the first 1000 years and (b) the period between year 1000 and year 5000.

$$\begin{aligned}
 Q_{ao} &= K_r(T_r - T_1) = K_r(T_r - T_s) + K_r(T_s - T_1) \\
 &= F_{\text{spin}} + K_r(T_s - T_1). \quad (12)
 \end{aligned}$$

Equation (12) states that although the heat flux is the same as in the spinup, the ocean will drift from T_s . Further, as K_r decreases, the SST is freer to evolve from the modeled climatology. An examination reveals that in both run 1 and run 2, salinity (especially SSS) also drifts from that of the spinup, in response to changes in convection pattern.

b. Change of thermal damping from a spinup under mixed boundary conditions

In order to further test this hypothesis of the inevitability of the drift we have also carried out another experiment, designated run 3. It starts from a steady state of a second spinup RF (Table 2), which is forced by mixed boundary conditions, with a salt flux diagnosed also from RR. The model under mixed boundary conditions has similar overturning circulations to those shown in Fig. 2 owing to the weak

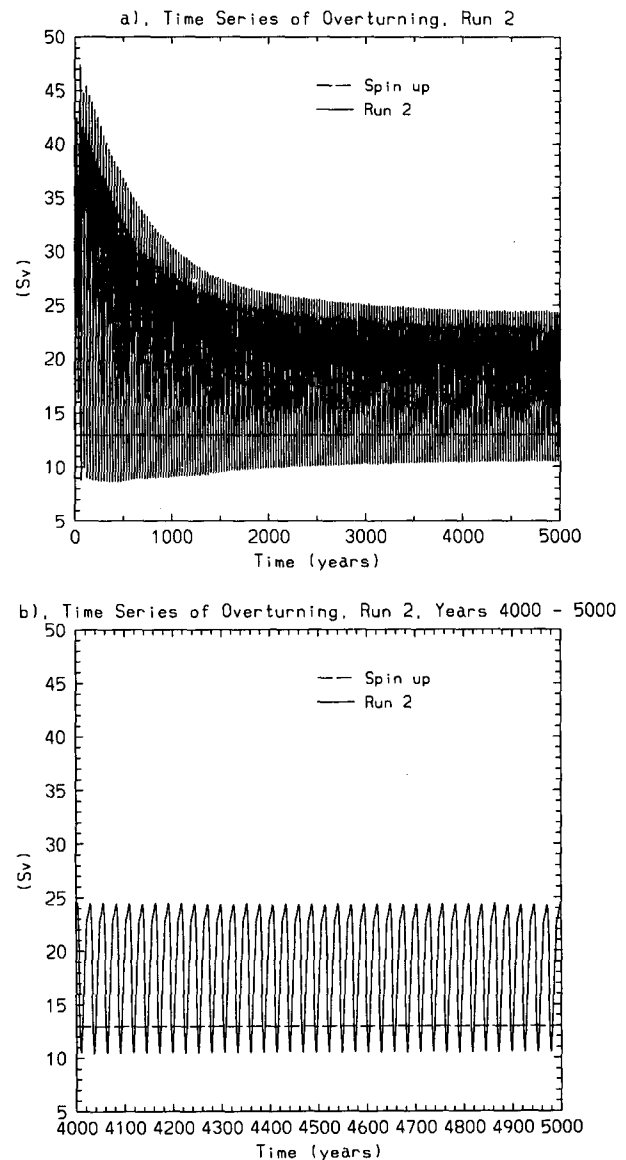


FIG. 4. Time evolution of the northern overturning (in Sverdrups) at 64°N , 2350 m for run 2, that is, with a thermal damping of $9.875 \text{ W m}^{-2} \text{ K}^{-1}$ and a restoration on surface salinity, for (a) period between year 0 and year 5000 and (b) a magnification covering the period between year 4000 and year 5000.

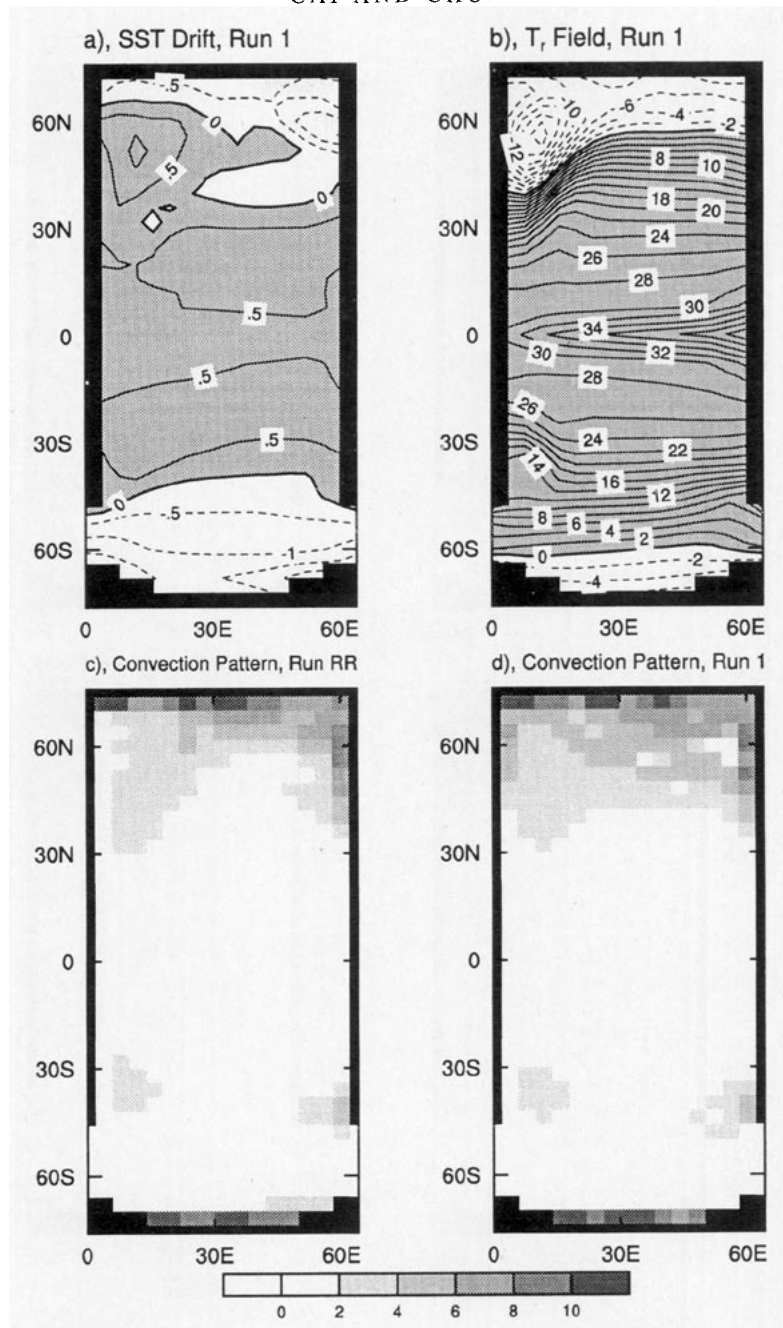


FIG. 5. (a) SST drift for run 1. The drift is the difference between an average over the last 10 years of run 1 and the steady state of run RR. (b) T , field used to drive run 1. (c) and (d) convection patterns (i.e., the locations and intensity of convections) of the steady state of run RR and run 1, respectively. The intensity is shown by the penetration depth in terms of model levels, indicated by the legend.

restoration for SSS (Tziperman et al. 1994; Cai 1996a). The thermal forcing condition is then switched to one the same as that of run 2, and the flux forcing for salinity remains. Drift and variability occur (Fig. 7) similar to those in run 2 but with a period of 27 years. The oscillation amplitude de-

creases somewhat owing to the “braking” effect of salinity because SSS is free to respond. Figure 8 shows the difference fields of SST and SSS between the mean over the last 10 steady oscillation cycles and the initial state. Indeed, substantial SSS drift occurs, even though only the thermal damping alters.

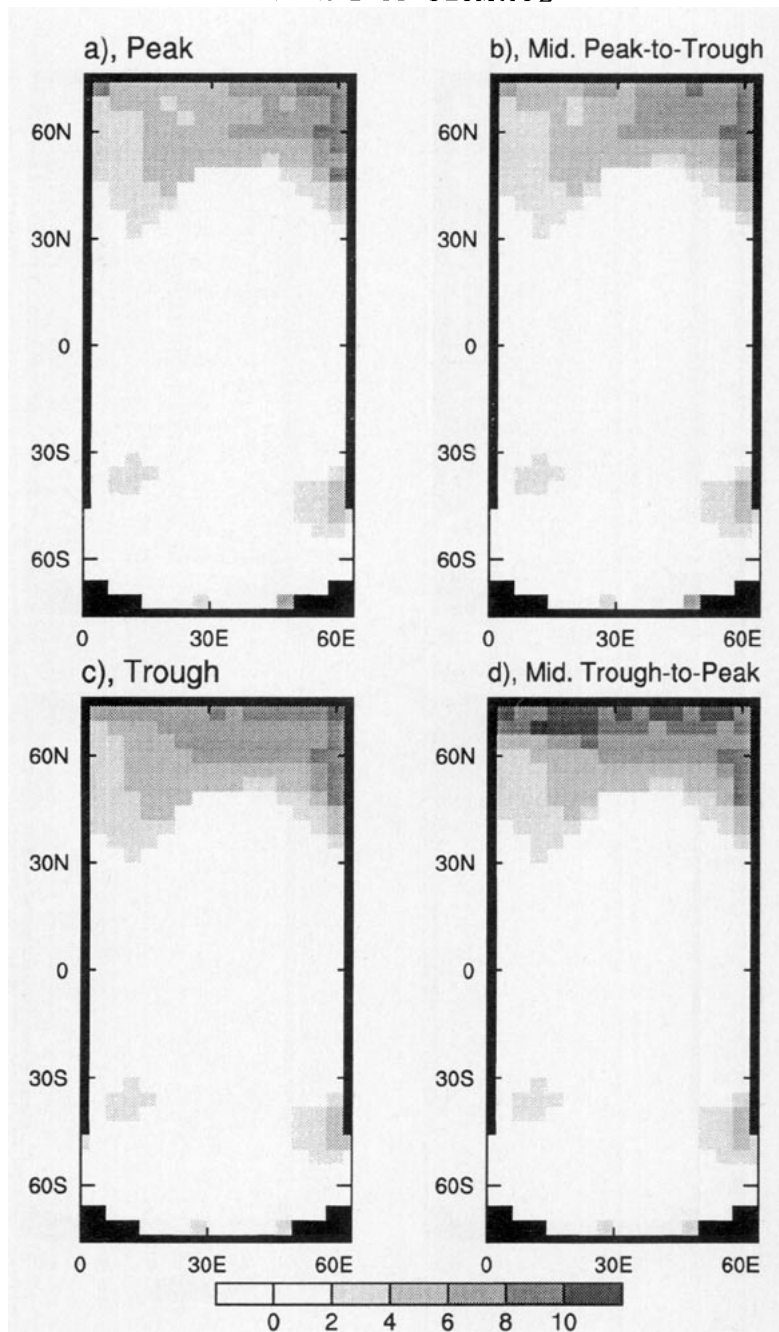


FIG. 6. Convection pattern at a quarter period interval for run 2 corresponding to times when the overturning in Fig. 3b is at (a) a maximum and (b) at a minimum.

c. Change of thermal damping from a spinup under a thermal forcing only

We have also carried out experiments in which salinity is kept constant and uniform at 34 ppt. Initially, the model is spun up to a steady state by restoring the model surface temperature to that given in Fig. 1a using a $K_H = 79 \text{ W m}^{-2} \text{ }^\circ\text{C}^{-1}$. This run is referred to as run R0 (Table 2). Runs 4 and 5 start from the

steady state of R0, with a K , of 39.5 ($\alpha = 0.5$) and 26.3 ($\alpha = 0.33$) $\text{W m}^{-2} \text{ }^\circ\text{C}^{-1}$, corresponding to a damping timescale of 30 and 45 days, respectively (Table 2). The model is integrated for a further 11 000 years. Drift takes place in both runs, and in run 5 interdecadal oscillations with a period of 27.1 years persist (Fig. 9). Comparing runs 3 and 5, we note that persistent oscillations are more easily generated in run 5. This is because in run 5 the braking

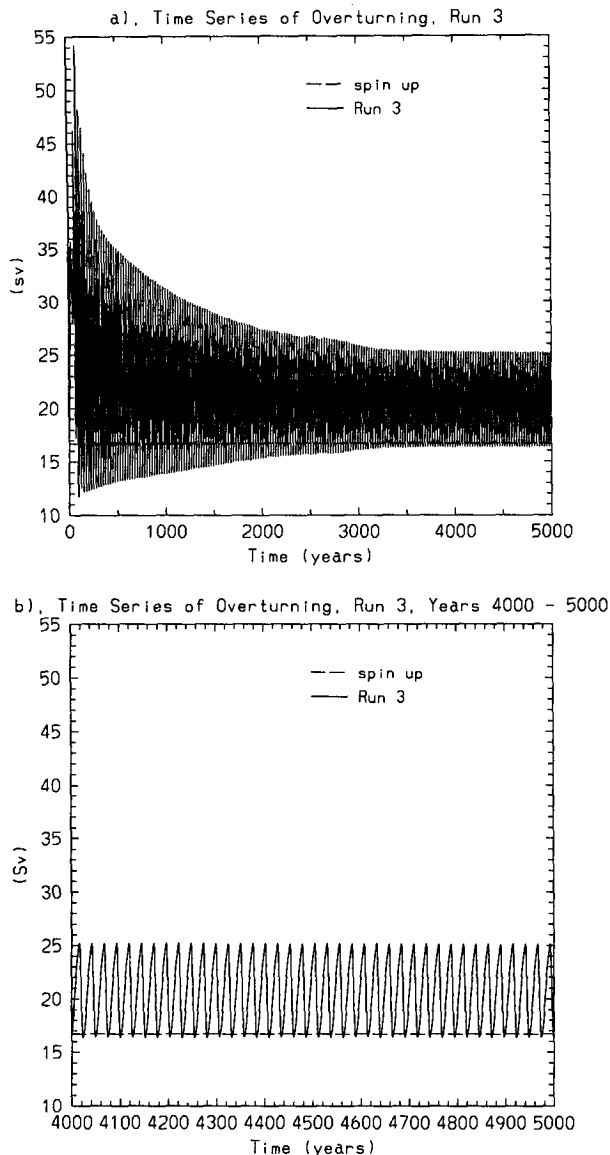


FIG. 7. Time evolution of the northern overturning (in Sverdrups) at 64°N , 2350 m for run 3, which starts from a steady state of a run (run RF) under mixed boundary conditions. From the steady state of RF, the thermal forcing condition is diagnosed using a thermal damping rate of $9.875 \text{ W m}^{-2} \text{ K}^{-1}$: (a) the period between year 0 and year 5000 and (b) a magnification covering the period between year 4000 and year 5000.

effect of salinity is absent [see Greatbatch and Zhang (1995) and Cai et al. (1996b) for a discussion].

4. Discussion

Before we proceed to discuss the relevance of these model results to the coupled atmosphere–ocean modeling, it is useful to address several issues. First, during our spinups (runs RR, RF, or R0) we use a thermal

damping rate of $79 \text{ W m}^{-2} \text{ }^{\circ}\text{C}^{-1}$, a rate about twice that commonly used. To study the possible effect of this large initial damping, we have conducted runs that continue from spinups under a thermal damping rate of $39.5 \text{ W m}^{-2} \text{ }^{\circ}\text{C}^{-1}$. We find that although the magnitude of the drift varies with the extent of the change in thermal damping, the major features described above appear. That is, as the thermal damping weakens, drift occurs; as the thermal damping weakens further, internal variability takes place.

Second, the design of the experiments may favor a substantial drift and a vigorous oscillation when the thermal damping weakens. In our study, a simple model is run with zonally averaged restoring thermohaline conditions, which are derived from observations. Such a simple approach renders that one has no way of knowing a priori whether these restoring conditions could be compatible with the OGCM. It is reasonable to argue that models with realistic basin configuration and bottom topography would have a better likelihood of being compatible with the restoring conditions since these restoring conditions are based on a realistic system. Although this may be true, we believe that incompatibility generally exists. We know that the observed forcing conditions are not perfect; even if the OGCM is state of the art, the model physics do not fully represent that in the real world. Deficiencies in model dynamic processes, either absent, poorly parameterized, or not accommodated by the model resolution, mean that there is incompatibility. Therefore, drift and oscillation will occur once the incompatibility is allowed to manifest itself, although the intensity of these features varies with the extent of the incompatibility.

Third, in the presence of any incompatibility, convection in the spinup state is intermittent. That the instability of a convection pattern plays a significant role in the generation of drift and oscillations raises a question as to how the model results depend upon the model convection scheme. To address this question, we have repeated run RR (a spinup) and run 1 using the convection scheme of Rahmstorf (1993). The advantage of the scheme over that of Cox (1987) is that it achieves complete mixing when a vertical instability occurs. We found that upon switching to weaker thermal damping, the model behaves in a way similar to that in run 1.

Finally, as commented in section 3a, a flux correction for a coupled model is usually diagnosed by averaging the flux fields over a period of several years. In order to ensure an identical heat flux at the moment of the switch, this is not carried out in the experiments described above. To test the possible effect, we have repeated run 1 using a heat flux diagnosed by averaging over the final 10 years of the spinup. The general time-dependent behavior and final state of the model hardly differ from those in the original run 1. Thus, we conclude that the effect of averaging the heat flux is neg-

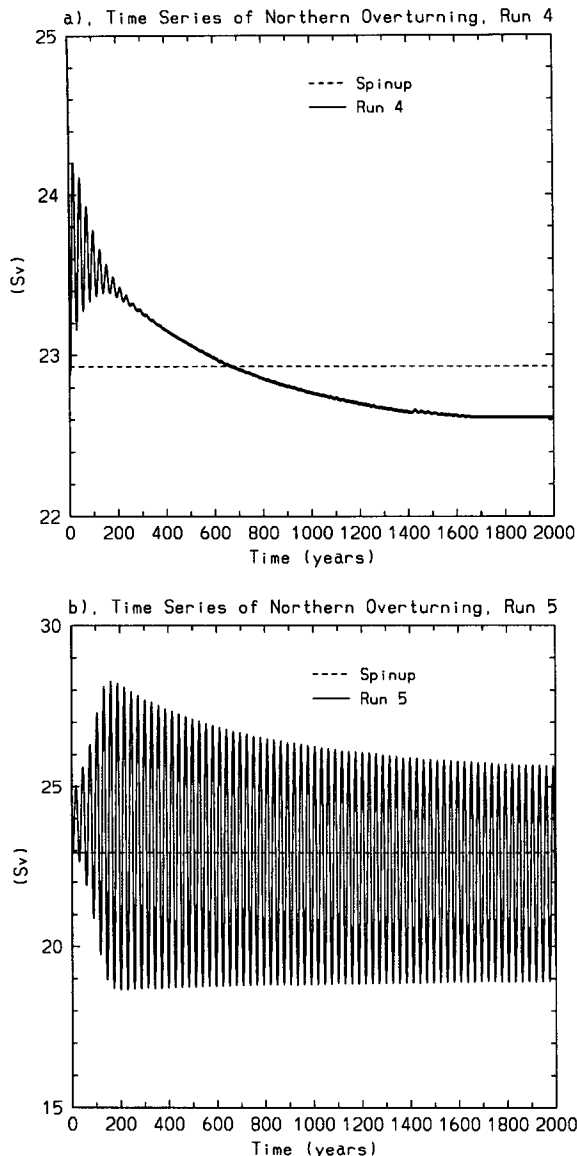


FIG. 9. Time evolution of the northern overturning (in Sverdrups) at 64°N , 2350 m for runs 4 and 5. Both start from the steady state of a run (run R0) under a thermal forcing only. The thermal forcing conditions are diagnosed from the steady state using damping rate 39.5 (run 4) and 26.33 (run 5) $\text{W m}^{-2} \text{K}^{-1}$.

Most of the precoupling spinups for atmosphere–ocean coupled models are carried out by restoring model SST and SSS to Levitus climatologies. These spinups will have problems obtaining a perfect steady state, especially when the model resolution is coarse. In these models, it is not clear whether the given climatologies can be maintained by model dynamics. As pointed out by Moore and Reason (1993), in areas characterized by sharp fronts in the climatologies, models experience problems maintaining strong fronts such as those observed because the large horizontal eddy

diffusivities in the model constantly try to eliminate them. This means that in these regions, the climatologies are not compatible with the model. In the presence of such incompatibility, the model convection in the spinup steady state is intermittent, and the atmospheric heat and/or freshwater transport implied in the diagnosed heat and freshwater fluxes are not a perfect match with the oceanic heat/freshwater transports. Cai (1995) has demonstrated that such a mismatch can generate interdecadal oscillations when the diagnosed fluxes are used to force the model.

A flux correction diagnosed from such a spinup bears the imprint of the incompatibility, which is, upon coupling, permanently present in the subsequent simulations. As discussed above, this may become the cause of drift and variability. On the other hand, there is no dynamical reason why in coupled models the heat flux from the model atmosphere to the model ocean should always match the oceanic dynamics. For example, the heat flux is influenced by many atmospheric processes, which are weakly dependent or even completely independent of the ocean (Cai et al. 1995; Cai 1995). At this stage, however, it is not entirely clear what generates the oscillations in the existing fully coupled models (e.g., Delworth et al. 1994; GOF). In our model, this incompatibility is carried over to the new system via the constant flux term in (11) (see §2), and the incompatibility then drives the drift and the oscillation.

That the convection pattern changes with the thermal damping raises questions regarding the validity of the flux correction as diagnosed from a restoring spinup. It is tempting to argue that the correction should perhaps be derived from a more realistic simulation. For example, run 3 is performed using a more realistic damping rate, and therefore the flux correction should be diagnosed from such a run. This new flux correction will be rather different from that diagnosed from the spinup, because it has to maintain a different convection pattern. This may reduce the drift somewhat, but since the thermal forcing condition of this run is diagnosed from the spinup, it still inherits the incompatibility. Further, if the diagnosed correction has to adjust for the maintenance of incompatibility-driven oscillations, it would need to be time dependent, varying on the timescale of the oscillation. This is not only impractical but also has the effect of preconditioning an oscillatory signal. It follows that an ultimate reduction of incompatibility-induced drift and variability can only be achieved by improving model dynamics and the quality of climatologies.

Acknowledgments. Wenju Cai is supported by the Australian Department of Environment, Sport, and Territories. Peter Chu is supported by the Office of Naval Research High Latitude, Physical Oceanography, and Naval Ocean Modeling and Prediction Programs. Peter Baines, Kevin Walsh, and Barrie Hunt reviewed an early draft of the paper. Reviewers provided construc-

tive comments. Harvey Davies provided the plotting routines for the figures. This work was made possible by GFDL for making the MOM code available.

REFERENCES

- Bryan, F., 1986: High-latitude salinity effects and interhemispheric thermohaline circulation. *Nature*, **323**, 301–304.
- , 1987: Parameter sensitivity of primitive equation ocean general circulation models. *J. Phys. Oceanogr.*, **17**, 970–985.
- Bryan, K., 1969: A numerical method for the study of the circulation of the World Ocean. *J. Comput. Phys.*, **4**, 347–376.
- , 1984: Accelerating the convergence to equilibrium of ocean–climate models. *J. Phys. Oceanogr.*, **14**, 666–673.
- Cai, W., 1994: Circulation driven by observed surface thermohaline fields in a coarse resolution ocean general circulation model. *J. Geophys. Res.*, **99**, 10 163–10 181.
- , 1995a: Interdecadal variability driven by mismatch between surface flux forcing and oceanic freshwater/heat transport. *J. Phys. Oceanogr.*, **25**, 2643–2666.
- , 1995b: Global present-day ocean climate and its stability under various surface thermohaline forcing conditions derived from Levitus climatology. *Progress in Oceanography*, Vol. 36, Pergamon, 219–247.
- , 1996a: The stability of NADWF under mixed boundary conditions with an improved diagnosed freshwater flux field. *J. Phys. Oceanogr.*, **26**, 1081–1087.
- , 1996b: Generation of thermal oscillation in an ocean model. *Quart. J. Roy. Meteor. Soc.*, in press.
- , and S. Godfrey, 1995: Surface heat flux parameterizations and the variability of thermohaline circulation. *J. Geophys. Res.*, **100**, 10 679–10 792.
- , and R. J. Greatbatch, 1995: Compensation for the NADW outflow in a global ocean general circulation model. *J. Phys. Oceanogr.*, **25**, 226–241.
- , and P. G. Baines, 1996: Interactions between thermohaline and wind-driven circulations and their relevance to the dynamics of the Antarctic Circumpolar Current in a coarse resolution global OGCM. *J. Geophys. Res.*, **101**, 14 073–14 093.
- , R. J. Greatbatch, and S. Zhang, 1995: Interdecadal variability in an ocean model driven by a small, zonal redistribution of the surface buoyancy flux. *J. Phys. Oceanogr.*, **25**, 1998–2010.
- Cox, M. D., 1987: GFDL Ocean Model Circular No. 7. GFDL/Princeton University, Princeton, NJ, 1 pp.
- Cubasch, U., K. Hasselmann, H. Höck, E. Maier-Reimer, U. Mikolajewicz, B. D. Santer, and R. Sausen, 1994: Time-dependent greenhouse computations with a coupled ocean–atmosphere model. *Climate Dyn.*, **8**, 55–69.
- Delworth, T., S. Manabe, and R. J. Stouffer, 1993: Interdecadal variations of the thermohaline circulation in a coupled ocean–atmosphere model. *J. Climate*, **6**, 1933–2011.
- Dickinson, R. E., 1981: Convergence rate and stability of ocean–atmosphere coupling schemes with a zero-dimensional climate model. *J. Atmos. Sci.*, **38**, 2112–2120.
- Gill, A. E., and K. Bryan, 1971: Effects of geometry on the circulation of a three-dimensional Southern-Hemisphere ocean model. *Deep-Sea Res.*, **18**, 685–721.
- Gordon, H. B., and E. O’Farrell, 1996: Transient climate change in the CSIRO coupled model with dynamic sea ice. *Mon. Wea. Rev.*, in press.
- Greatbatch, R. J., and S. Zhang, 1995: An interdecadal oscillation in an idealized ocean basin forced by a constant heat flux. *J. Climate*, **8**, 81–91.
- , and K. A. Paterson, 1996: Interdecadal variability and oceanic thermohaline adjustment. *J. Geophys. Res.*, **101**, in press.
- Griffies, S. M., and E. Tziperman, 1995: A linear thermohaline oscillator driven by stochastic atmospheric forcing. *J. Climate*, **8**, 2440–2453.
- Haney, L. R., 1971: Surface boundary condition for ocean circulation models. *J. Phys. Oceanogr.*, **1**, 241–248.
- Holland, W. R., 1973: Baroclinic and topographic influences on the transport in western boundary currents. *Geophys. Fluid Dyn.*, **4**, 187–210.
- Huang, R. X., 1994: Thermohaline circulation: Energetics and variability in a single hemisphere basin model. *J. Geophys. Res.*, **99**, 12 411–12 421.
- , and L. Chou, 1994: Parameter sensitivity study of the saline circulation. *Climate Dyn.*, **10**, 391–409.
- Hughes, T. M. C., and A. J. Weaver, 1994: Multiple equilibria of an asymmetric two-basin ocean model. *J. Phys. Oceanogr.*, **24**, 619–637.
- Manabe, S., and R. J. Stouffer, 1993: Century-scale effects of increased atmospheric CO₂ on the ocean–atmosphere system. *Nature*, **364**, 215–218.
- , and ———, 1994: Multiple century response of a coupled ocean–atmosphere model to an increase in atmospheric carbon dioxide. *J. Climate*, **7**, 5–23.
- Marotzke, J., 1989: Instability and multiple steady states of the thermohaline circulation. *Oceanic Circulation Models: Combining Data and Dynamics*, D. L. T. Anderson and J. Willebrand, Eds., Kluwer, 501–511.
- , 1990: Instabilities and multiple equilibria of the thermohaline circulation. Ph.D. thesis, Berlin Institute Meereskunde Kiel, 126 pp.
- , 1994: Ocean models in climate problem. *Ocean Process in Climate Dynamics: Global and Mediterranean Examples*, P. Malanotte-Rizzoli and A. R. Robinson, Eds., Kluwer Academic, 79–109.
- , and J. Willebrand, 1991: Multiple equilibria of the global thermohaline circulation. *J. Phys. Oceanogr.*, **21**, 1372–1385.
- Mikolajewicz, U., and E. Maier-Reimer, 1994: Mixed boundary conditions’ in OGCMs and their influence on the stability of the model’s conveyor belt. *J. Geophys. Res.*, **99**, 22 633–22 644.
- Moore, A. M., and C. J. C. Reason, 1993: The response of a global OGCM to climatological surface boundary conditions for temperature and salinity. *J. Phys. Oceanogr.*, **23**, 300–328.
- , and H. B. Gordon, 1994: An investigation of climate drift in a coupled atmosphere–ocean–sea ice model. *Climate Dyn.*, **10**, 81–95.
- Pacanowski, R. C., K. W. Dixon, and A. Rosati, 1991: GFDL Modular Ocean Model, users guide version 1.0. GFDL Ocean Group Tech. Rep. No. 2, 46 pp.
- Power, S. B., 1995: Climate drift in a global ocean general circulation model. *J. Phys. Oceanogr.*, **25**, 1025–1036.
- , and R. Kleeman, 1993: Multiple equilibria in a global ocean general circulation model. *J. Phys. Oceanogr.*, **23**, 1670–1680.
- , A. M. Moore, D. A. Post, N. R. Smith, and R. Kleeman, 1994: Stability of North Atlantic Deep Water formation in a global ocean general circulation model. *J. Phys. Oceanogr.*, **24**, 904–916.
- Rahmstorf, S., 1993: A fast and complete convection scheme for ocean models. *Ocean Model.*, **101**, 9–11.
- , and J. Willebrand, 1995: The role of temperature feedback in stabilizing the thermohaline circulation. *J. Phys. Oceanogr.*, **25**, 787–805.
- Randall, D. A., and Coauthors, 1992: Intercomparison and interpretation of surface energy fluxes in atmospheric general circulation models. *J. Geophys. Res.*, **97**, 3711–3724.
- Sausen, R., and F. Lunkeit, 1990: Some remarks of the cause of climate drift of the coupled ocean–atmosphere models. *Beitr. Phys. Atmos.*, **63**, 141–146.
- , K. Barthel, and K. Hasselmann, 1988: Coupled ocean–atmosphere models with flux correction. *Climate Dyn.*, **2**, 145–163.
- Schopf, P. S., 1983: On equatorial waves and El Niño. II: Effects of air–sea thermal coupling. *J. Phys. Oceanogr.*, **13**, 1878–1893.

- Tziperman, E., J. R. Toggweiler, Y. Feliks, and K. Bryan, 1994: Instability of the thermohaline circulation with respect to mixed boundary conditions: Is it really a problem for realistic models? *J. Phys. Oceanogr.*, **24**, 217–232.
- Wajsowicz, R. C., and A. E. Gill, 1986: Adjustment of the ocean under boundary forces. Part I: The role of Kelvin waves. *J. Phys. Oceanogr.*, **16**, 2097–2114.
- Weaver, A. J., and E. S. Sarachik, 1991a: The role of mixed boundary conditions in numerical models of the ocean's climate. *J. Phys. Oceanogr.*, **21**, 1470–1493.
- , and ———, 1991b: Evidence for decadal variability in an ocean general circulation model: An advective mechanism. *Atmos.–Ocean*, **29**, 197–231.
- Winton, M., 1996: The role of horizontal boundaries in parameter sensitivity and decadal-scale variability of coarse-resolution ocean general circulation models. *J. Phys. Oceanogr.*, **26**, 289–304.
- Zhang, S., R. J. Greatbatch, and C. A. Lin, 1993: A reexamination of the polar halocline catastrophe and implications for coupled ocean–atmosphere models. *J. Phys. Oceanogr.*, **23**, 287–299.